



## SEISMIC HAZARD ANALYSIS AND ROCK GROUND MOTIONS FOR A SITE IN DUBAI

Ayman A Shama<sup>1</sup>

### ABSTRACT

The seismic design criteria for a new bridge in Dubai require that the bridge satisfies an operational performance for the 475-year return period earthquake, and life safety performance for the 2475-year return period earthquake. The site is located at Dubai Creek on the west coast of the United Arab Emirates at 25 12' 47" latitude and 55 20' 48" longitude. Ground motions for use in time history dynamic analysis of the structure were developed for the two seismic hazards on the basis of site specific seismic hazard analysis that considered all the seismic sources. The probabilistic seismic hazard analysis (PSHA) indicated that the peak ground acceleration for the 475-year return period earthquake is 0.17g and 0.33g for the 2475-year return period earthquake. This paper summarizes the PSHA and the development of the rock ground motions.

### Introduction

The site intended for this investigation is the proposed location for a new arch bridge that will be located at Dubai Creek on the west coast of the United Arab Emirates at 25 12' 47" latitude and 55 20' 48" . The main objective of the present study was to develop the rock ground motions for both the design earthquake (475-year return period) and the maximum considered earthquake (2475-year return period). These earthquakes were required for the performance based seismic design of the bridge. In pursuit of this objective, probabilistic seismic hazard analysis was conducted that counted for all the seismogenic sources that affect the site. The hazard spectra of the seismic hazard analysis were then employed for the simulation of the ground motions.

### Overview of the Seismic Hazard Analysis

Probabilistic seismic hazard analysis (PSHA) expresses the hazard in terms of the annual frequency of exceedance. Several models were developed for ground motion occurrences during the past decades. Nevertheless, the Poisson model [Cornell, 1968] is considered a standard and was employed by the United States Geological Survey for the development of the seismic hazard maps of US. This model, which is adopted in this study, assumes that earthquakes occur independently in a fixed time period wherein the probability of exceedance  $P(z)$  of a ground motion level  $z$  occurring in a design time period  $t$  at the site is related to the annual frequency of

---

<sup>1</sup>Seismic Engineering Specialist, Parsons, 100 Broadway, New York, NY 10005-1983

ground motion exceedance at the site  $\gamma(z)$  by:

$$P(z) = 1 - e^{(-\gamma(z) t)} \quad (1)$$

The total frequency  $\gamma(z)$  is made up of contributions from each independent source and expressed as:

$$\gamma(z) = \sum_N \left[ \sum_M \lambda(m_i) \sum_R P(Z > z \setminus m_i, r_j) P(R = r_j \setminus m_i) \right]_n \quad (2)$$

where  $\sum_N \sum_M \sum_R$  = summations over all (N) seismic sources, (M) earthquake magnitudes, and (R) distances to fault rupture respectively;  $\lambda(m_i)$  = the annual frequency of occurrence of earthquake magnitude  $m_i$  above a minimum size on seismic source  $n$ ;  $P(Z > z \setminus m_i, r_j)$  = the probability that ground motion level  $z$  will be exceeded given an earthquake of magnitude  $m_i$  on source  $n$  at a distance  $r_j$  from the site; and  $P(R = r_j \setminus m_i)$  = the probability that an earthquake occurs on source  $n$  at a certain distance  $r_j$  from the site with magnitude  $m_i$ .

The rate of occurrence of earthquake  $\lambda(m_i)$  is obtained by recurrence laws for different magnitudes. Both the truncated exponential recurrence model and the Characteristic earthquake model were employed in the present study as will be shown for each seismic source in the subsequent sections. The conditional probability of exceeding a ground motion level for a certain earthquake magnitude and distance  $P(z > Z \setminus m_i, r_j)$  is obtained from ground motion attenuation models selected for the site as discussed below. The distance probability distribution  $P(R = r_j \setminus m_i)$  depends on the geometry of earthquake sources and their locations with respect to the site. It is usually assumed that earthquakes occur with equal likelihood on different parts of a source. The distance probability distribution function also incorporates the magnitude dependence of earthquake rupture size. The methods of its implementation are basically empirical relying on field observations after past earthquakes for calibrating models. In the present study the following two relationships by Wells and Coppersmith (1994) were employed:

$$\text{Log}(L) = -2.44 + 0.59 M_w \quad (3)$$

$$\text{Log}(W) = -1.01 + 0.32 M_w \quad (4)$$

where  $L$  is the subsurface rupture length in km,  $W$  is the rupture width in km, and  $M_w$  is the moment magnitude.

## Logic Trees

The probability formulation in equations (1) and (2) includes the inherent variability in the physical parameters associated with the earthquake and seismic waves. These formulations, however, does not include the uncertainties associated with the selection of other model parameters, such as the appropriate attenuation relationships for a particular site, the maximum

magnitude, the slip rate, etc. These epistemic uncertainties can be directly incorporated within the analysis framework to include their effects on the hazard curve by logic trees [Coppersmith and Youngs (1986)]. The logic tree approach considers potential alternative source parameters and assigns an associated weighting factor to the potential alternative. McGuire (2004) found that the most three critical seismicity parameters to estimate correctly for a successful seismic hazard analysis are the attenuation model, the maximum magnitude, and the slip rate (activity rate). Logic trees were used in this study to model the epistemic uncertainties associated with fault parameters.

### Representation of Seismic Sources

The following seismic sources were considered in the analysis on the basis of the tectonic settings of the region of interest: (1) Zagros fold-thrust region; (2) Makran subduction zone; (3) Zendan-Minab-Palami fault system; and (4) local crustal faults in UAE including Dibba, Wadi El Fay, Wadi Ham, Wadi-Shimal, Oman, and West Coast. Figure 1 illustrates an overall seismic setting of Dubai.



Figure 1. Overall seismic setting of Dubai

### Attenuation Models

Since there is no specific attenuation relationship for UAE, the present probabilistic study employed attenuation models that represent worldwide records from earthquakes having attenuation characteristics similar to the intended region in this study. Three attenuation models were used for Zagros fold-thrust region, which is characterized by numerous blind thrust faults. The attenuation model by Ambraseys et al. (1996) was selected since it is based on ground motion records from Europe and Middle East, particularly Iran; the attenuation model by Abrahamson and Silva (1997) for rock sites was also selected since it is based on a database of 655 recordings from 58 earthquakes occurred worldwide; and the model by Boore-Joyner-Fumal (1997) was selected as it is based on ground motions that occurred in Western United States such as southern California, which exhibits similar seismic activity to Zagros thrust zone. The models by Atkinson and Boore (2003), Gregor et al. (2002), and Youngs et al. (1997) were selected for

the Makran subduction zone. These models were validated against ground motion records from subduction zones worldwide. The attenuation models by Ambraseys et al. and Abrahamson-Silva were selected for Minab fault and the local faults of UAE besides the rock attenuation equation by Campbell (2003) for Eastern United States as it represents a stable region with low rate of seismicity as these regions. The West Coast fault, however, employed the Campbell-Bozorgnia near-source attenuation equation (Campbell and Bozorgnia, 2003) to include the near source effects for earthquakes in the vicinity of Dubai. The attenuation models by Campbell and Campbell-Bozorgnia were based on worldwide ground motions. Earlier versions of these models were employed in a seismic hazard assessment study for Iran (Tavakoli et al., 1999). It is important to note that the attenuation models were assigned with equal credibility to every seismic source.

### Zagros Fold-Thrust Region

The Zagros-Fold-Thrust Region is characterized by numerous blind thrust faults and hence was represented as an area source model, where historical seismicity was used to define the source's parameters. A region of the Zagros fold-thrust at the southern parts of the Persian Gulf as shown in Figure 2a was selected for this investigation. The earthquake catalogue of the International Institute for Earthquake Engineering and Seismology in Iran [IIEES, 2002] was employed for the assessment of the seismic historical activity of this region. The truncated exponential recurrence model (McGuire and Arabasz, 1990) was employed to represent the magnitude distribution, which is illustrated in Figure 2b with the parameters used in the seismic hazard analysis.

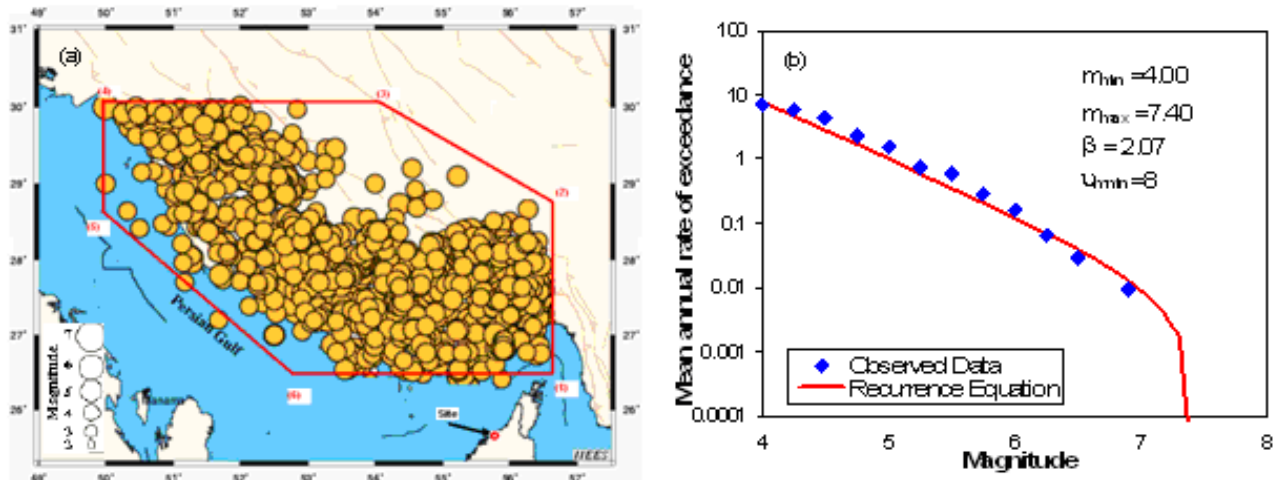


Figure 2. Seismicity of the Zagros-fold thrust region: (a) Seismic activity; and (b) Truncated exponential magnitude distribution

### Makran Subduction Zone

The Makran subduction zone as shown in Figure 3 exhibits a strong difference in behavior between its east and west parts. The plate boundary in the eastern part has ruptured in the past in

large thrust earthquakes. On the contrary, in western part intraslab earthquakes up to  $M_s$  6.5 occurred within the subducted slab at depths of around 60 km [Byrne and Sykes (1992)]. Consequently, in the present study a portion representing the deformation front of western Makran between 24.96 latitude, 57.62 longitude and 23.95 latitude, 60.53 longitude was considered.

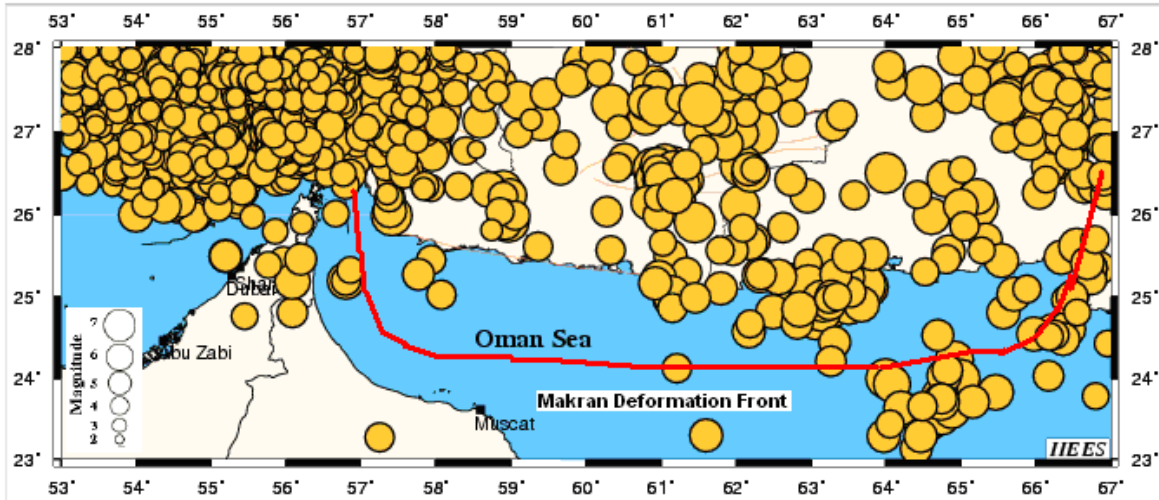


Figure 3. Seismicity of the western segment of Makran subduction zone: (a) location; and (b) seismic activity

A characteristic earthquake model was adopted and magnitude-rupture length relationships by Wells and Coppersmith (1994) were employed to estimate the magnitudes for three potential scenarios of segmentation: (i) a 150 km rupture length that corresponds to rupture of single segment; (ii) a 250 km rupture length that represents the average length of the rupture of two adjacent segments; and (iii) a 400 km rupture length representing the rupture of the entire portion of western Makran considered in the study. The estimates of the maximum magnitude which ranged from 7.8 to 8.6 were implemented in the logic tree for this source to represent the uncertainty in the maximum magnitude. A slip rate of 30 mm/year [Regard et al. 2005] was taken as a best estimate and assumed to be uncertain by a factor of  $\pm 20\%$ , which is typical for this parameter. The logic tree for the Makran subduction zone is displayed in Figure 4.

### **Zendan-Minab-Palami Fault System**

The Zendan-Minab-Palami (ZMP) fault system is the transition that accommodates the differential velocity between the Zagros continental collision zone and the Makran oceanic subduction. The seismicity of this fault system is illustrated in Figure 5, which displays the epicenters of the earthquakes above moment magnitude 5 that occurred in this region (25.5N latitude-56.0E longitude, and 28.25N latitude-58.25E longitude) between April, 1964 and May, 2007 [IRIS (2008)]. A recent tectonic analysis [Regard et al. 2005] suggested a right-lateral strike-slip motion of  $10 \pm 3$  mm/yr of the whole system. This value was adopted as best estimate for the slip rate with  $\pm 30\%$  uncertainty. A value of  $M_w = 6.5$  was selected as a best estimate for the maximum magnitude with uncertainty  $\pm 0.5$ .

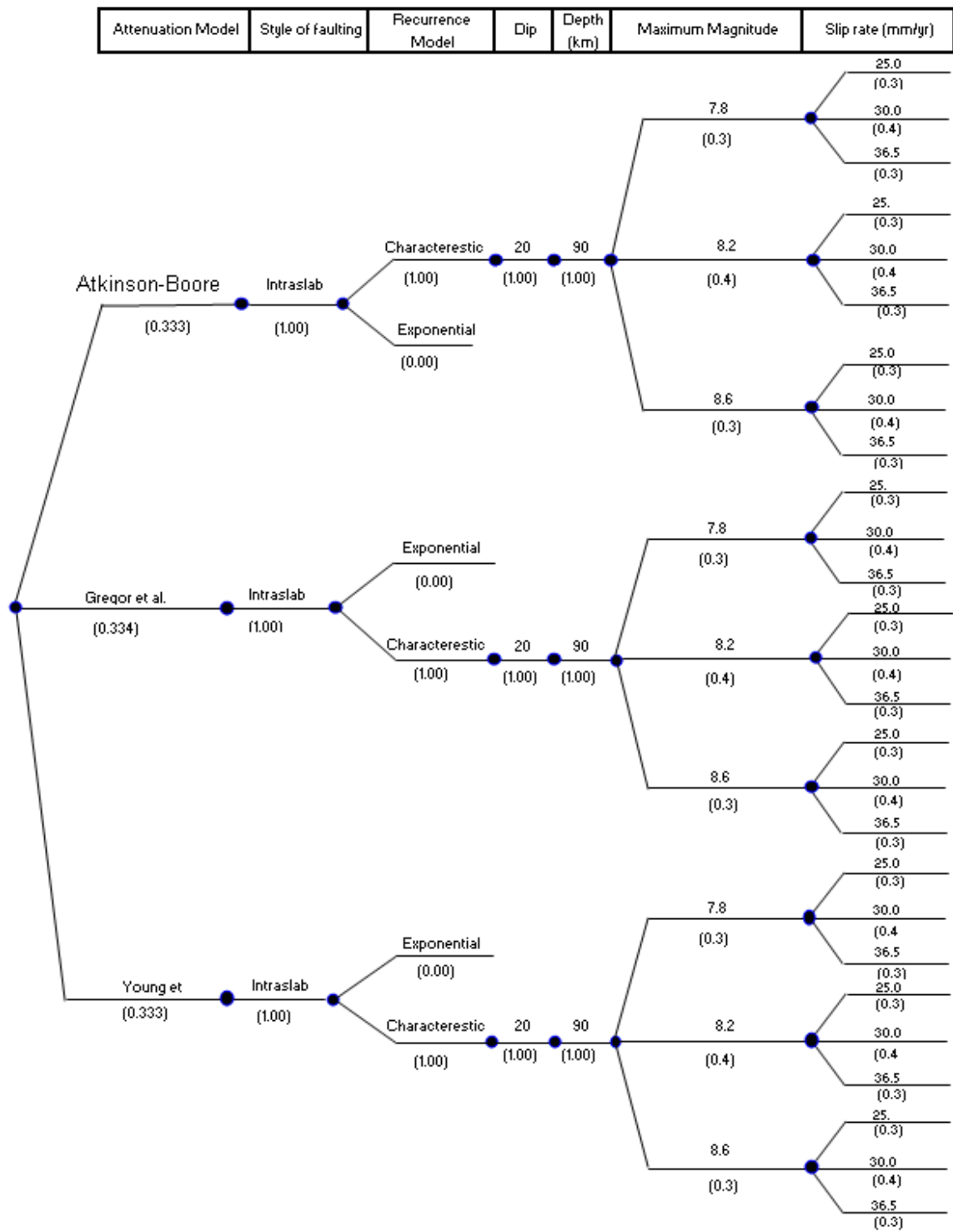


Figure 4. Example of a logic tree for the western segment of the Makran subduction zone





Figure 5. Seismicity of the Zendan-Minab-Palami fault system

### Local Faults in UAE

Local faults in UAE consist of the Dibba fault zone, the Oman Mountains faults, and the West Coast fault. A study by Rodgers et al. (2002) reported a right-lateral strike-slip faulting mechanism for the Dibba line and normal fault mechanism for other faults of the Dibba fault zone. Remote sensing investigations on Oman Mountains [Kusky et al (2005)] revealed two major fault sets extend for tens of kilometers, identified to be north-northwest normal faults and cut through Tertiary rocks in the Mountains. The West Coast fault is a left-lateral strike slip fault that has been reported on the tectonic map of the Arabian Peninsula (Johnson, 1998). It was included in earlier studies for UAE (Wyss and Al-Homoud, 2004; Mwafy et al., 2006), and hence included in the present study as a potential seismic source.

Since the information about the seismic parameters of these faults are very scarce a criteria was developed to implement them in the present study. First, the latitude/longitude coordinates for the faults were inferred from the literature (Rodgers et al., 2006; Ziegler, 2001; and Johnson, 1998). Next, earthquake catalogues of the incorporated Research Institutions for Seismology (IRIS, 2008) were searched for reported seismic events in UAE from 1973 to 2008.

The results are illustrated in Figure 6, which depicts the earthquakes with  $M_w$  greater or equal to 4. It is observed that the seismic faults particularly the West coast can be correlated to some of these events. From this database, best estimates of the activity rate and the maximum magnitude for each fault were determined and an average depth of 15 km was adopted. The activity rate associated with each fault was then converted to a slip rate using procedures by McGuire, 2004 and logic trees were established for all faults.

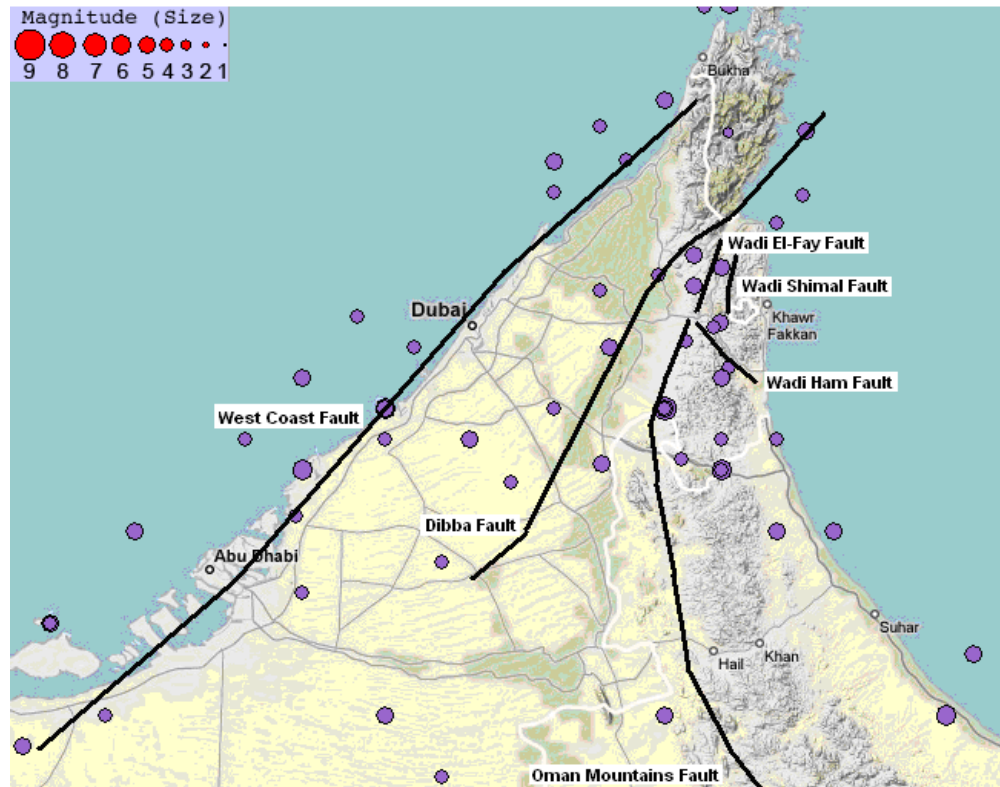


Figure 6. Seismic activity of local faults in UAE from 1973 to 2008( $M_w \geq 4.0$ )

### Results of PSHA

The PSHA was conducted for response spectral values covering a range of vibration periods up to 10 seconds. The analysis was conducted by EZ-FRISK version 7.26 (Risk Engineering, 2008). Figure 7 illustrates the hazard contribution from the individual seismic sources for the peak ground acceleration (PGA). It is shown that the West Coast fault dominates the hazard at ground motions of about 0.1 g and greater. It is also shown that both the Zagros fold-thrust region and Zendan-Minab-Palami fault system dominate the low ground motion levels of the hazard (i.e. ground motions less than 0.1 g). This observation is corroborated by the fact that Northern UAE is not currently affected by the frequent earthquakes of magnitude  $\leq 5.5$   $M_w$  occurring annually at the Zagros fold-thrust region since attenuation of the seismic waves from this source will result in inconsequential ground motion levels.



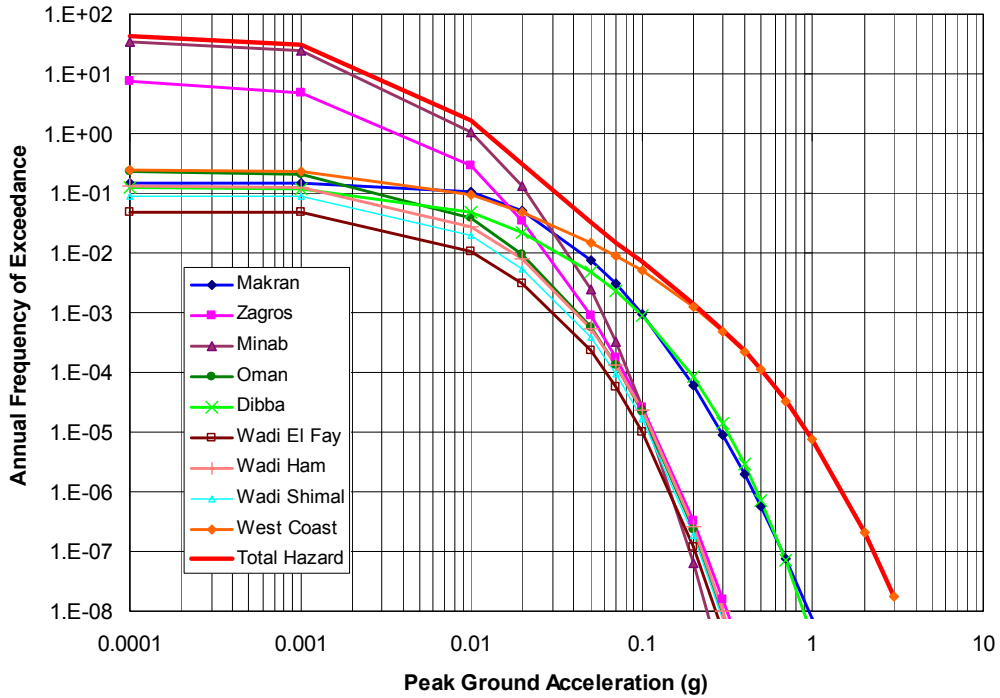


Figure 7. Contributions to the PGA hazard for each seismic source

To illustrate the contributions of events in various magnitude and distance intervals, Figure 8 shows the deaggregation of PGA hazard at 0.2 g by magnitude and distance. As shown in Figure 8a earthquakes of average magnitude of 5.4 dominate the hazard. This is the range of potential earthquakes from both the west coast fault and Dibba fault. It is also shown that earthquakes of magnitudes in the range of 6 to 7 have a very low contribution to the hazard since earthquakes of such magnitudes are likely to occur at the Zagros fold-thrust region, which is not dominating the high ground motion levels of the hazard. It is also observed that the earthquakes of magnitudes in the range of 7 to 8.5 have considerable contribution to the total hazard. These are the potential characteristic earthquakes at the Western Makran subduction zone. Figure 8b shows that the near fault (West Coast) earthquakes are dominating the hazard.

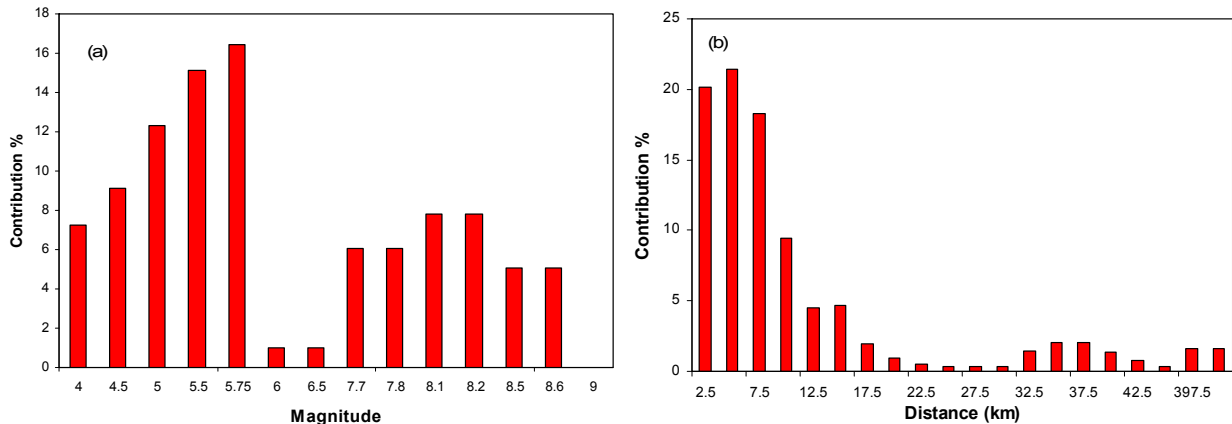


Figure 8. Deaggregation of PGA hazard at 0.20g: (a) by magnitude; and (b) by distance

Figure 9a shows the hazard curves for peak ground accelerations and for 5 percent-

damped spectral ordinates at six selected periods of vibrations for the site of interest. These are the basis of the uniform hazard spectra for the site. The spectra developed using this procedure are uniform in the sense that they have the same probability of exceedance at each frequency of vibration. These spectra for bedrock are displayed in Figure 9b for both the 475-year return period and the 2475-year return period. It is observed that the peak ground acceleration for the 475-year return period spectrum is 0.17 g, and 0.33 g for the 2475-year return period spectrum, which agrees with previous seismic hazard studies for this region [Abdalla and Al-Homoud (2004)].

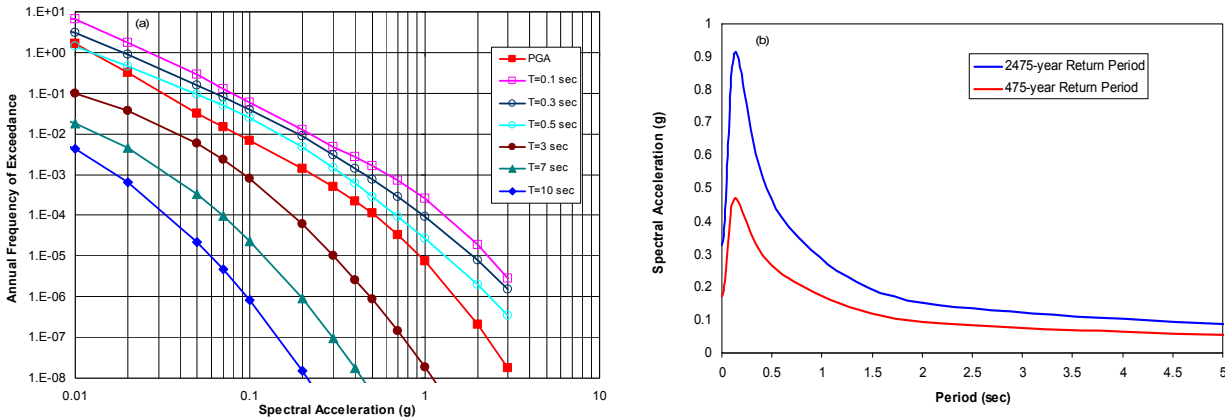


Figure 9. Development of the hazard spectra: (a) hazard curves for a range of periods; and (b) uniform spectra for return periods of 475 and 2475 years

### Development of Rock Ground Motions for the Site

The two bedrock hazard spectra obtained from the PSHA study were employed for the development of the site's rock ground motions. The spectral matching technique was used for this purpose. This method scales the Fourier amplitude spectrum of a known record for a range of periods to each of the hazard spectra, while preserving the phase spectrum of the original record contingent that the selected records are consistent with the hazard spectrum in terms of magnitude and epicentral distance. Hence, the produced ground motion matches the PGA and the frequency content of the hazard spectrum. On such basis, three known rock records were selected for spectral matching to obtain the rock ground motions for the seismic design of the bridge; each represents one of the dominant seismic sources.

Ground motion-1 is the Chalfant record of the Adobe Hills earthquake occurred in California, September, 2004. This earthquake had a 5.4 seismic moment and the hypocentral distance at Chalfant station was 46.4 km. Therefore it was selected for spectral matching to represent a potential earthquake at one of the local faults in Northern UAE. Ground motion-2 is the Rapel record of the Valparaiso earthquake occurred in Chile, March, 1985. This event had a surface wave magnitude of 7.2 and the hypocentral distance at Rapel was 108.2 km. It was selected for spectral matching to represent a potential earthquake at the Western Makran subduction zone as it occurred on a similar zone in South America. Ground motion-3 is the Bandar-Abas record of the Qeshm Island Earthquake of Iran occurred in November, 2005. This

earthquake had a magnitude of 5.9 and was selected for spectral matching to represent a potential event in the Persian Gulf or the Zagros zone. Representative ground motions of the longitudinal components of motions 2 and 3 for the 2475-year hazard are depicted in Figure 10.

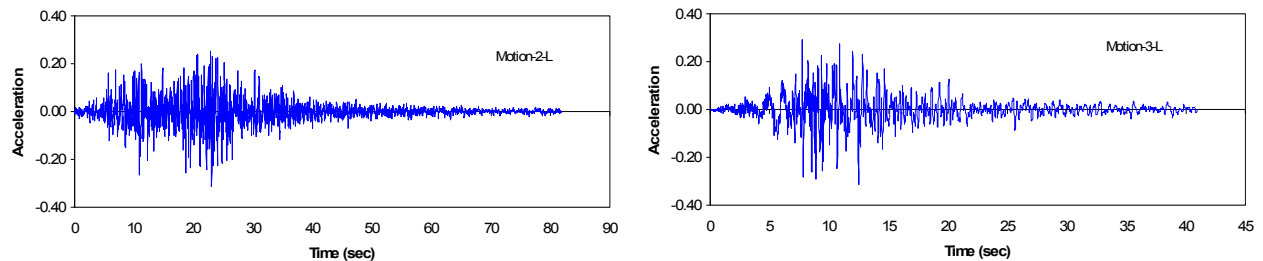


Figure 10. Simulated ground motions: longitudinal components of motions 2 and 3

## Conclusions

This paper presented the study involved in the development of the rock ground motions for a site in Dubai, UAE located at Dubai Creek on the west coast of the United Arab Emirates. A probabilistic site specific seismic hazard analysis was conducted first to establish the hazard spectra for two seismic hazard levels representing both the 475-year return period and 2475-year return period earthquakes. The PSHA considered all the seismogenic sources including the western Makran subduction zone, the Zagros fold-thrust region, Zendan-Minab-Palami fault system; and local crustal faults in UAE. The study showed that the local faults particularly the west coast fault dominate the hazard the peak ground acceleration for the 475-year return period spectrum is 0.17 g, and 0.33 g for the 2475-year return period spectrum. The hazard spectra were employed for the development of the rock ground motions using the spectral matching technique.

## Acknowledgments

The author would like to thank Mr. Kenneth Serzan Vice President of Parsons Transportation Group for the valuable discussions throughout the course of this investigation.

## References

- Abdalla, J.A., and AL-Homoud, A.S., 2004. Seismic hazard assessment of United Arab Emirates and its surroundings, *Journal of Earthquake Engineering*; 8 (6) 817-837.
- Abrahamson, N.A. and Silva, W.J., (1997), "Empirical response spectral attenuation relations for shallow crustal earthquakes," *Seismological Research Letters*, 68 (1) 94-127.
- Ambraseys, N. N. Simpson, K. A., Bommer, J. J., (1996), "Prediction of horizontal response spectra in Europe," *Earthquake Engineering and Structural Dynamics* 25, 371-400.
- Berberian, M., (1995), Master "blind" thrust faults hidden under the Zagros folds: active basement tectonics and surface morphotectonics" *Tectonophysics* 241, 193-224.
- Boore, D.M. Joyner, W.B. Joyner and T.E. Fumal (1997), "Equations for estimating horizontal response spectra and peak acceleration from Western North American earthquakes: A summary of recent work," *Seismological Research Letters*, 68 (1), 128-153.
- Byrne, D.E., Sykes, L.R., and Davies, D.M., 1992. Great thrust earthquakes and seismic slip along the plate boundary of the Makran subduction zone, *Geophysical Research*, 97,449-478.

Cornell, C.A., 1968. Engineering seismic risk analysis, Bulletin of Seismological Society of America, 58(5):1583-1606.

Campbell, K.W. (2003). "Prediction of strong ground motion using the hybrid empirical method and its use in the development of ground-motion (attenuation) relations in Eastern North America.", Bulletin Seismological Society of America, 93 (3), 1012-1033.

Campbell, K.W. and Y. Bozorgnia (2003), "Updated near-source ground motion (attenuation) relations for the horizontal and vertical components of peak ground acceleration and acceleration response spectra," Bulletin Seismological Society of America, 93 (1), 314-331.

Coppersmith, K.J. and Youngs, R.R. (1986). "Capturing uncertainty in probabilistic seismic hazard assessments with intraplate tectonic environments," Proceedings, 3<sup>rd</sup> U.S. National Conference on Earthquake Engineering, Charleston, South Carolina, pp.301-312

EZ-FRISK-7.26, 2008. A program for earthquake ground motion estimation, Risk Engineering Inc, Boulder, CO USA.

IIEES, 2008. International Institute of Earthquake Engineering and Seismology, <http://www.iiees.ac.ir>

IRIS, (2008). Incorporated Research Institutions for Seismology, Washington, DC <http://www.iris.edu>

Johnson, P.R., 1998. Tectonic map of Saudi Arabia and adjacent areas, Deputy Ministry for Mineral Resources Technical Report USGS-tr-98-3 (IR-948)

Kusky, T., Robinson, C, and El-Baz, F., 2005. Tertiary-Quaternary faulting and uplift in northern Oman Hajar Mountains, Journal of the Geological Society, 162,871-888.

McGuire, R.K. and Arabaz, W.J., 1990. An introduction to probabilistic seismic hazard analysis Geotechnical and Environmental Geophysics, Volume 1.

McGuire, R.K., 2004. *Seismic hazard and risk analysis*. EERI Monograph MNO-10.

Mwafy, A., El Nashai, A., Sigbjornsson, R., and Salama, A., 2006. Significance of severe distant and moderate close earthquakes on design and behavior of tall buildings, Structural Design of Tall Buildings, 15,391-416.

Regard, V., Bellier, O., Thomas, J., Bourles, and Feghhi, K., 2005. Cumulative right-lateral fault slip rate across the Zagros-Makran transfer zone: role of the Minab-Zendan fault system in accommodating Arabia-Eurasia convergence in southeast Iran, Geophys. J. Int., 162, 177-203.

Rodgers, A., Fowler, A., Al-Amri, A., and Al-Enezi, A., 2006. The March 11, 2002 Masafi, United Arab Emirates earthquake: Insights into the seismotectonics of the northern Oman Mountains, Tectonophysics 414, 57-64.

Tavakoli, B., Ashtiany, M.G., 1999. Seismic hazard assessment of Iran, Annali Di Geofisica, 42 (6), 1013-1021.

Wells, D.L. and K.J. Coppersmith, 1994. New empirical relationships among magnitude, rupture length, rupture width, rupture area, and surface displacement. Bull. Seis. Soc. Am. 84(4): 974-1002.

Wyss, M., and Al-Homoud, A., 2004. Scenarios of seismic risk in the United Arab Emirates, an approximate estimate. Natural Hazards; 32:375-393

Youngs, R.R., Chiou, S.J., Silva, W.J., Humphrey, J.R. (1997), "Strong ground motion attenuation relationships for subduction zone Earthquakes," Seismological Research Letters, 68 (1), 58-73.

Ziegler, M., 2001. Late Permian to Holocene paleofacies evolution of the Arabian plate and its hydrocarbon occurrences, GeoArabia, Vol. 6, No. 3, 2001